Design and Analysis of Clover Leaf Shaped Fractal Antenna Integrated With Stepped Impedance Resonator for Wireless Applications

SATHEESHKUMAR PALANISAMY (skcommn@gmail.com)
Coimbatore Institute of Technology https://orcid.org/0000-0002-9267-4381
Balakumaran T
Coimbatore Institute of Technology

Research

Keywords: clover leaf, FR4 substrate, harmonics suppression, aperture-coupled, semi-fractal ring, stepped impedance resonator

Posted Date: February 3rd, 2022

DOI: https://doi.org/10.21203/rs.3.rs-1279989/v1

Design and analysis of Clover Leaf Shaped Fractal Antenna integrated with Stepped Impedance Resonator for wireless applications

SATHEESHKUMAR PALANISAMY*,
Faculty, Coimbatore Institute of Technology, Coimbatore.
BALAKUMARAN.T,
Faculty, Coimbatore Institute of Technology, Coimbatore.
*Corresponding Author mail id: skcommn@gmail.com

***Abstract*—** A novel multi-band clover leaf shaped fractal antenna with integrated filtering to reduce higher order harmonics has been proposed. Existing microstrip filtering antennas endure limited gain, narrow impedance bandwidth, and undesired frequency radiations. The proposed antenna is designated to operate simultaneously in following operating bands: 3.35–3.6 GHz for WiMAX, 5.156–5.825 GHz for WLAN, 5.7–6.4 GHz for Intelligent Transport Systems-ITS, and 7.7–8.5 GHz for ITU-R applications. The proposed patch is realized by combining two semi fractal ring microstrip patches like the geometry of a three-leaf clover with dual layered Stepped Impedance Resonator(SIR) integrated at bottom layer of the second substrate. The SIR band pass filter exhibits odd and even modes suppresses higher order harmonics and undesired radiations. An aperture coupled feeding in the proposed patch offers better bandwidth and impedance matching. The number of iterations is increased to get the desired multiband characteristics. The proposed microstrip fractal antenna has the geometrical dimensions of 50 × 50 × 2 mm^3. It is observed that, both the simulated and measured results offers peak gain of > 5dBi and better return loss (S_{11}) i.e., 3.3–3.6 GHz band offers S_{11} of -33.73dB, (5.15-5.825) GHz band offers S_{11} of -36.69dB , (5.795-6.4) GHz band shows the S_{11} of -36.25 dB and for (7.725-8.5) GHz, the return loss is -33.209 dB. Harmonics at 6.42GHz ($1.8f_0$), 7.37GHz ($1.5f_0$) and 9.04GHz($1.73f_0$) has been suppressed and shows linear polarization in the WLAN band and circular polarization in the ITU-R and WiMAX bands.

***Index Terms*—**clover leaf, FR4 substrate, harmonics suppression, aperture-coupled, semi-fractal ring, stepped impedance resonator.

I. INTRODUCTION

With the advent of wireless communication technologies, the network capacity of the channel is growing, and the speed of transmission is increasing, this makes the operating system more flexible, which makes the bands of operation keep growing. From the development of the Global system of mobile communication to the fourth generation (4G) wireless communication system and from WiMAX to WLAN network standards, it is important to have antennas that are both small and multiband. The fractal concept is a new technique for the designing patch antenna similar to the use of self-similar possessions of the fractal geometry for realizing the multiband characteristics, by the use of space-filling assets so as to decrease the antenna dimensions[1]. The radiating characteristics of the micrrostip patch antenna are altered on a regular basis by employing self-similar shapes, space-filling performance and increasing the utilization rate of space. As a result, the antenna's effective electrical geometrical dimensions is increased, the antenna's surface current path is maximized and bandwidth gets increased. Variety of fractal structure styles are available, each of which provides multiple design options for new antenna geometries that will shine in future application scenarios. Various methods for designing fractal antennas are shown in references [2–3], including a combination of Sierpinski Carpet and Giusepe Peano[4], octagon iterations[5], bandpass frequency selective surface array structure [6], and slotted quasi-fractal [7]. Another important parameter in efficient radiation is better impedance bandwidth, which can be achieved by varying substrate thickness, feeding techniques and multiple resonators [8]. Improvement in bandwidth or antenna dimensions results in signal degradation due to mutual impedance properties. As a result, a dielectric material with high thickness, less effective dielectric constant and varying feeding method is

preferred as it ensembles broader bandwidth with better gain and directivity. After analyzing various power feeding techniques, aperture coupling improves parameters such as directivity, gain, efficiency, bandwidth and return loss with VSWR<2[9]. Therefore, aperture coupling feeding technique is the best way to improve the radiation mechanism. Aperture coupling is a multi-layer coupled feeding technique separating radiating patch from the feed. A slot(aperture) is positioned in the ground plane that is shared by the two dielectric substrate layers, allowing energy coupled between the layers. The microstrip antenna serves as both a radiator and a filter in the active RF circuits. However, if the patch is not properly designed to suppress undesired spurious emission and harmonic resonances, such microstrip antenna can results in harmful electromagnetic radiation, affecting overall performance of the communication systems. An extra filter is inserted between the amplifier and the microstrip patch antenna to overcome this issue[10, 11].The introduction of a conventional filter, on the other hand, will affect the antenna's fundamental operating frequency and impedance matching property, potentially degrading system performance significantly. Furthermore, the filter geometry is bulk and resistant to integration and miniaturization. To address the issue, alternative methods such as the use of Photonic Band Gap(PBG) structures [12], stubs for tuning [13], Defective Ground Structure(DGS) [14], and hybrid new structures [15] has been implemented. Horii and Tsutsumi employ 2-D PBG structures to suppress harmonic formation in a patch antenna, and suppressing third harmonics has been employed[16]. Furthermore, third harmonic suppression was achieved by properly positioning the tuning stub at the feed line [17–18]. DGS has gained popularity in recent years as another effective method of suppressing harmonic radiation in microstrip patch antennas [19, 20]. However, it remains challenging to achieve suppressing higher-order harmonics in a microstrip patch antenna using a single construction. In order to improve the suppression property, hybrid structures were developed, and suppressing upto fourth harmonics was accomplished[21,22]. [23] used a pair of a circular head open stub and circular headed dumbbell shaped DGSs to produce a low-pass filter that suppressed up to the fourth harmonic. [24] used a pair of half ring DGSs rather than a pair of circular headed dumbbell shaped DGSs, resulting in a 40% decrease in DGS area. Recently, it was proposed to suppress fifth harmonics using a pair of an inverted L-shaped stub and I-shaped DGSs and [25]. DGS, on the other hand, consumes considerable space. Additionally, the physical occupancy area of DGS is a critical factor to consider when building antennas, particularly in microwave integrated RF circuits. A smaller DGS occupancy area leaves more room for other devices to be integrated.

Methods/experimental:

The proposed antenna is designated to operate simultaneously in following operating bands: 3.35–3.6 GHz for WiMAX, 5.156–5.825 GHz for WLAN, 5.7–6.4 GHz for Intelligent Transport Systems-ITS, and 7.7–8.5 GHz for ITU-R applications. The proposed patch is realized by combining two semi fractal ring microstrip patches like the geometry of a three-leaf clover with dual layered Stepped Impedance Resonator(SIR) integrated at bottom layer of the second substrate. The SIR band pass filter exhibits odd and even modes suppresses higher order harmonics and undesired radiations. An aperture coupled feeding in the proposed patch offers better bandwidth and impedance matching. The number of iterations is increased to get the desired multiband characteristics. The proposed stacked clover leaf shaped fractal antenna integrated with stepped impedance filter possesses various outstanding features: (1) occupation area of fractal patch antenna decreasing considerably by 42% compared with the traditional one. (2) Harmonic suppression ranging from $2f_0$ to $4f_0$. (3) Better bandwidth covering all intended applications within the band along with improving radiation characteristics.

Literature Review

Numerous integrated harmonic suppression techniques are used to reduce the RF front end's complexity and occupancy volume. To create mismatching at the desired bands, short pins or aperture slots are introduced into the radiating patch [26]. In [27], Defected Ground structures (DGS) mitigates the impacts of harmonics. Harmonics are often suppressed further by positioning a band pass notch resonating filter nearer to the feeding[28]. However, the bulk of the techniques presented so far have addressed second-order harmonics, with higher-order harmonics receiving little attention. The narrow bandwidth in-band is another limitation of those works. Thanks to the space constraints, achieving multi-octave harmonic

suppression is usually difficult. In addition, combining the antenna and the filter can increase not only harmonic suppression but also boosts the frequency performance such as 10dB-bandwidth and frequency resonance. The antenna setup's bulkiness, on the other hand, increases the occupancy. In antenna arrays, many bandpass filtering design strategies have been employed and described in the literature. Feeding network like stub-loaded resonator (SLR) feeding network [29-30], microstrip and slotline transitions based feeding network [31], feedline and patchline coupling filtering feeding network [32], symmetrical Stepped Impedance Resonator(SIR) based feeding network [33], Radiating element of Jerusalem cross with a ring shaped aperture slot coupling feeding network [34], and a baluns connecting two power divider connected [35] feeding network are just a few examples. These filtering elements' passbands, on the other hand, are slender, with a passband bandwidth of 87.76% [31]. Furthermore, the resonating filter arrangement in [30] needs multi-layered structures to build numerous ports[33] and [34]. Hence, the complexity and size and of the filters, consequently increases the structural dimensions of the microstrip patch antenna. The use of SIRs in the construction of microstrip bandpass filters [36] with better stopband characteristics has been discovered to be beneficial. One of the most important characteristics of a Stepped Impedance Resonator is that its pass band frequencies may be modified by altering the parameters like high-low impedance ratio. This change causes, the first undesired harmonic can be significantly more than $2f_0$. For illustration, using an inductive effect, the design in [37] entirely suppresses the $2f_0$ resonance, and at the frequencies close to $3f_0$, the initial parasitic response is detected. A combination of several SIR structures can be employed to obtain a filter with a broad stopband [38]. Nonconventional SIRs [39] can be utilised to build efficient bandpass filters with spurious response control stop band over a wide range of frequencies. Generally, low-pass filters are incorporated with passband topologies in [40]. Harmonic resonances in distributed bandpass filtering network can be reduced by altering low-pass filtering network cutoff frequencies. Fractal patterns in nature intrigue and encourage scholars to examine them. Iteration Factor (IF) and Iteration Order (IO) are critical design parameters for framing fractal geometries (IF). A fractal geometry's iteration order is the number of iterations necessary to produce the specific fractal geometry, whereas the iteration factor is the scaling factor used in the specific iterations[41]. A significant growing field in antenna research is the creation of diverse structures of fractal antennas [42]. Wireless communication developments necessitate flexible antennas with tiny sizes and wideband or multiband capabilities to keep up with the times. A multilayer approach is offered in order to overcome various design limits, such as the realisable characteristic impedance values of the system.

A clover leaf shaped patch with a stepped impedance etched over the microstrip line make up the filtering network, which is modest. Although numerous microwave components with slotline approach have been recently examined [44], there has never been a report of a aperture(slotline) based filtering network for filtering antennas. In this scenario, the proposed fractal antenna has a wider harmonic-suppressed band and a higher bandwidth as compared to the works in [45]. The challenges of bulky dimensions, harmonics, bandwidth tradeoff with substrate thickness, and radiation characteristics are all overcome by a newly designed stacked clover leaf shaped fractal patch aperture coupled SIR filter antenna.

CONTRIBUTIONS

Generally, fractal geometry is accountable for radiating multiple band of frequencies comprising of lower order and higher order harmonics ($2f_0$,$3f_0$,$4f_0$….). This undesired harmonics reduces gain, return loss and other radiation characteristics of desired resonating frequencies. Thereby, stacking band pass filter network with the proposed fractal antenna will suppress the undesired harmonics and improves the peak gain, return loss and efficiency. Moreover, aperture coupled feeding is preferred over other feeding network because micro strip line and coaxial feed limits bandwidth by the order of 4-8% for every -10dB return loss.

This article proposes a unique compact aperture coupled four band stacked clover leaf fractal antenna with circular polarisation (CP). An arrangement of three-leaf clover fractal patch rings is employed to offer multiband capabilities. The proposed antenna covers a wide range of following operational frequencies: 3.35–3.6 GHz for WiMAX, 5.156–5.825 GHz for WLAN, 5.7–6.4 GHz for Intelligent Transport Systems-ITS, and 7.7–8.5 GHz for ITU-R. The WiMAX resonance band is related with the outer quasi clover shaped ring of fractal length. Quasi clover-shaped rings govern the resonance band for WLANs, while microstrip lines and clover leaves are used to create the ITU-R band. In the WiMAX and International Telecommunication Union Radiocommunication Sector(ITU-R) bands, the proposed antenna features circular polarisation (CP) characteristics, with CP bandwidths of 14% and 13%, respectively. Validation of the proposed approach is accomplished through simulations, and measurement reults. The uniqueness of the proposed structure is as follows, the proposed antenna achieves better reduction in occupancy size by 41% and offers better bandwidth

tradeoff with the substrate thickness by employing aperture coupling technique. The novel structure also offers better harmonics suppression, achieves peak gain of over 5dBi high percentage bandwidth, return loss of greater than -30dB and offers better impedance matching having the VSWR of <2.

ORGANIZATION

The residual segment of this approach is systematized as shown: section II is the depiction of a range of traditional methods associated with fractal antenna. Section III is the projected technique (clover leaf shaped fractal antenna design) portrayal, which is then followed by the performance analysis in section IV. At last, the overall conclusion is narrated in section V.

II. ANTENNA GEOMETRY AND EVOLUTION

This section is the deliberation of the proposed module in which the proposed mechanism is explained in a detailed manner. The stacked structure of the proposed antenna module is depicted in Fig.1

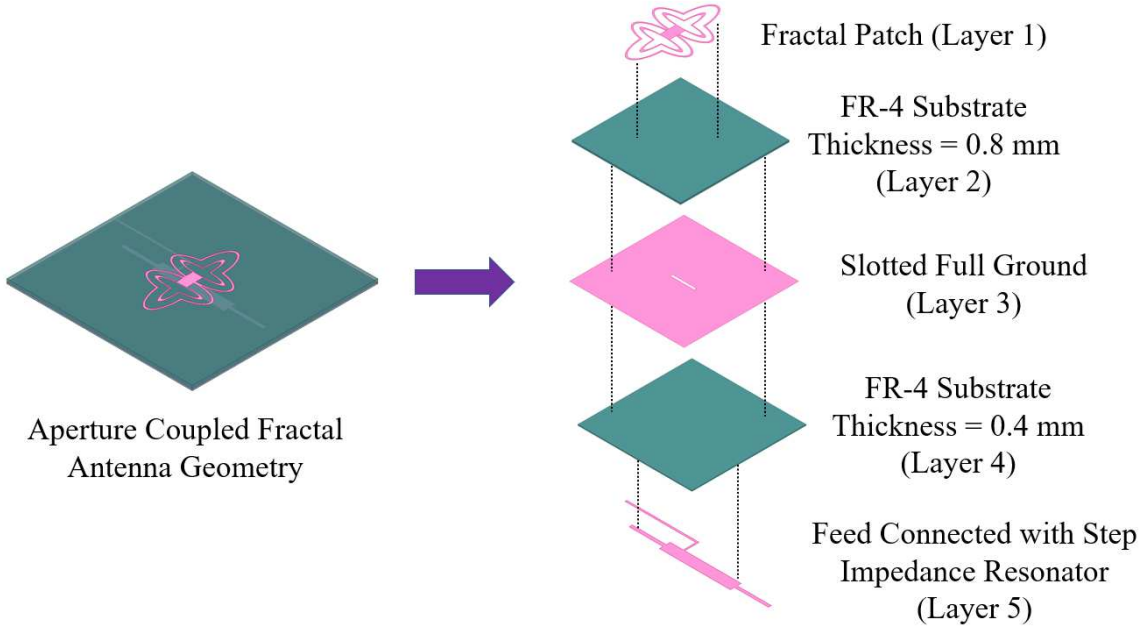

Fig.1 Layered structure of the proposed antenna

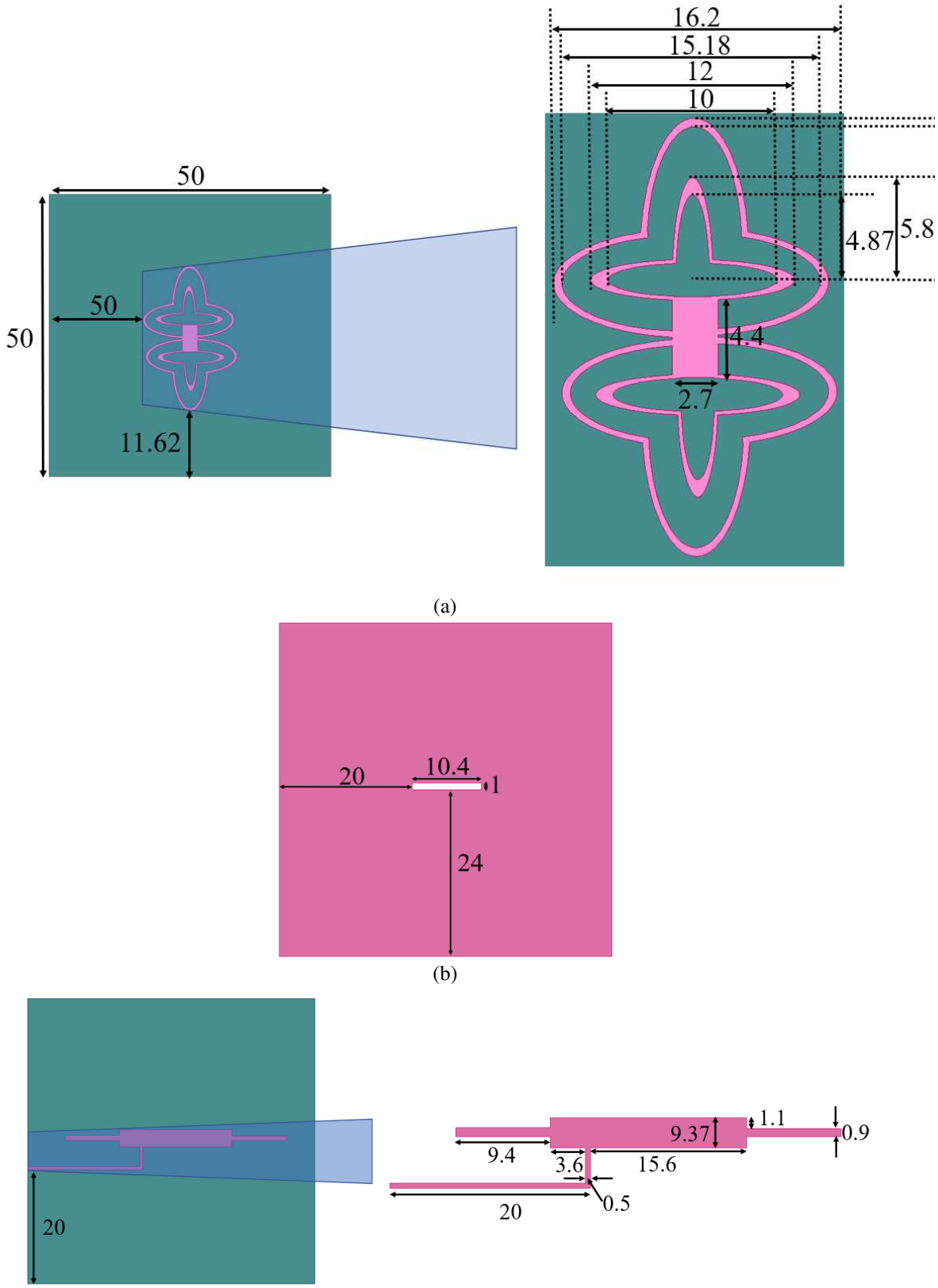

Fig 2. Antenna Geometry (a) Layered View (b) Layer 1 and 2 (c) Layer 3 (d) Layer 4 and 5

The proposed antenna's geometry and physical parameters are shown in Figure 2. A pair of Quasi-fractal rings similar to a three-leaf clover makes up the patch. To design a Stepped Impedance Resonator, a rectangular

structure with a dielectric constant =4.4, tan ð=0.024, and a thickness of the substrate=2 mm is etched on the printed circuit board (PCB)'s same side. The ground plane is etched to deploy aperture coupled feed with a width Wslot= 1 mm and a length Lslot= 10.4mm on a 50x50 mm^2 substrate. The Euclidean distance between the outer and inner semi fractal patches, as well as the microstrip line that connects the two quasi fractal rings, are critical to the antenna's multiband functioning.

Evolution of the antenna

Microstrip patch antennas are designed using regular geometries such as rectangles, squares, octagons, triangles, and circles. Aside from that, designing an antenna with a symmetrical geometry is preferred. The geometry of the proposed clover-leaf structure is as follows. Initially, the pattern is assumed to be a circle of radius (r = 15.875 mm). The different phases (iterations) of the proposed nature inspired fractal a structure is shown in Fig.3.

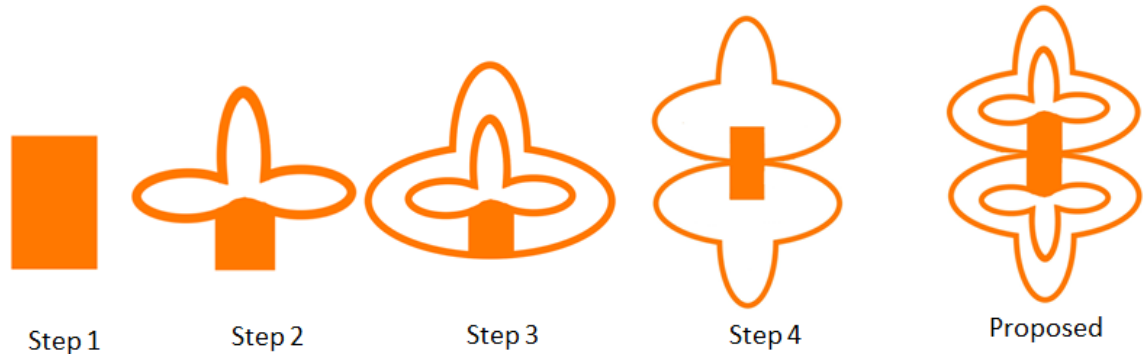

Fig 3. Evolution of proposed antenna

The minor (b) and major (a) axes of the pattern are scaled by 33% and 66%, and the resulting elliptical structures are cloned twice, resulting in a phase difference of 180^0 degrees and the development of a unique clover leaf.

$$a = r \times 66\% \quad (1)$$

$$b = r \times 33\% \quad (2)$$

The clover leaf has been scaled by 80%, resulting in inner compounded clover leaves. The microstrip line connects the two inner clover leaf phases separated by 180^0. The major (c) and minor (d) axes of an inner clover leaf are calculated as

$$a_1 = \frac{r}{4} \times 80\% \quad (3)$$

$$b_1 = \frac{r}{4} \times 10\% \quad (4)$$

In the elliptical patch antenna, the fields of radiation cause two modes that were upright to one another that have equal amplitude, however out of phase at 90 ˚. The feed position is located alongside the 45 ˚ line among the major and minor axis of the elliptical patch.

The four systematic steps considered in the design of the proposed antenna are shown below:

Step-1 (Ant.1): Constructing a rectangle patch to act as the trunk for connecting the inner clover ring patch , that dictates the WLAN and ITS bands' formation.

Step-2 (Ant.2): Add an inner ring patch in the form of a clover which facilitates the WiMAX band's formation.

Step-3 (Ant.3): At the ITU-R band, scaling the outer ring patch in the form of a clover covers the resonance mode.

Step-4(Ant 4): cloning the outer clover leaf by 180^0 to improve the response characteristics

Step-5(Proposed Antenna): cloning inner and outer clover leaf ellipse by 180^0 to get better resonance for four bands of WLAN, WiMAX, ITS and ITU-R bands simultaneously.

Fractal Length and Patch Radiating Area Calculation

As a result of the proposed fractal antenna implementation, the entire fractal radiating length gets expanded, and it now exceeds the traditional length of the proposed Microstrip patch in the form of a clover leaf. The customary length (C_L) of the suggested geometry is as follows:

$$C_L = 2\times (L_{P2} + W_{P2}) \qquad (5)$$

Two-leaf clover has the following fractal length:

$$F_{l1} = 8 \text{ x } \pi \text{ x } \sqrt{\frac{a^2 + b^2}{2}} \qquad (6)$$

$$F_{l2} = 8 \text{ x } \pi \text{ x } \sqrt{\frac{c^2 + d^2}{2}} \qquad (7)$$

The following formula is used to calculate the effective fractal length:

$$F_L = \sum_{n=1}^{2} F_{ln} \qquad (8)$$

The following formula is used to calculate the enhanced fractal length (EL):

$$E_L = \left(\frac{F_L - C_L}{C_L}\right) \text{x } 100\% \qquad (9)$$

The conventional area C_A of the proposed clover shaped antenna is

$$C_A = L_P \times W_P \qquad (10)$$

The fractal and conventional lengths of the proposed antenna are 162.3 and 92mm, respectively. The length of the effective fractal increases by 74.56% as a result. The fractal antenna's area is calculated as follows:

$$F_A = \pi \text{ x } [(8 \text{ x } m_1 \text{ x } m_2) + (7 \text{ x } m_3 \text{ x } m_4) - r_1^2]$$

The proposed geometry's radiating area (AR) is calculated as follows:

$$A_R = \left(1 - \frac{C_A - F_A}{C_A}\right) \text{x } 100\% \qquad (11)$$

The suggested antenna's computed effective fractal area is 347.32 mm^2. As a result, the suggested antenna's radiating area is approximately 96.22%. As a result, the proposed patch antenna's increased fractal length and maximum radiating area aid in obtaining better parametric results.

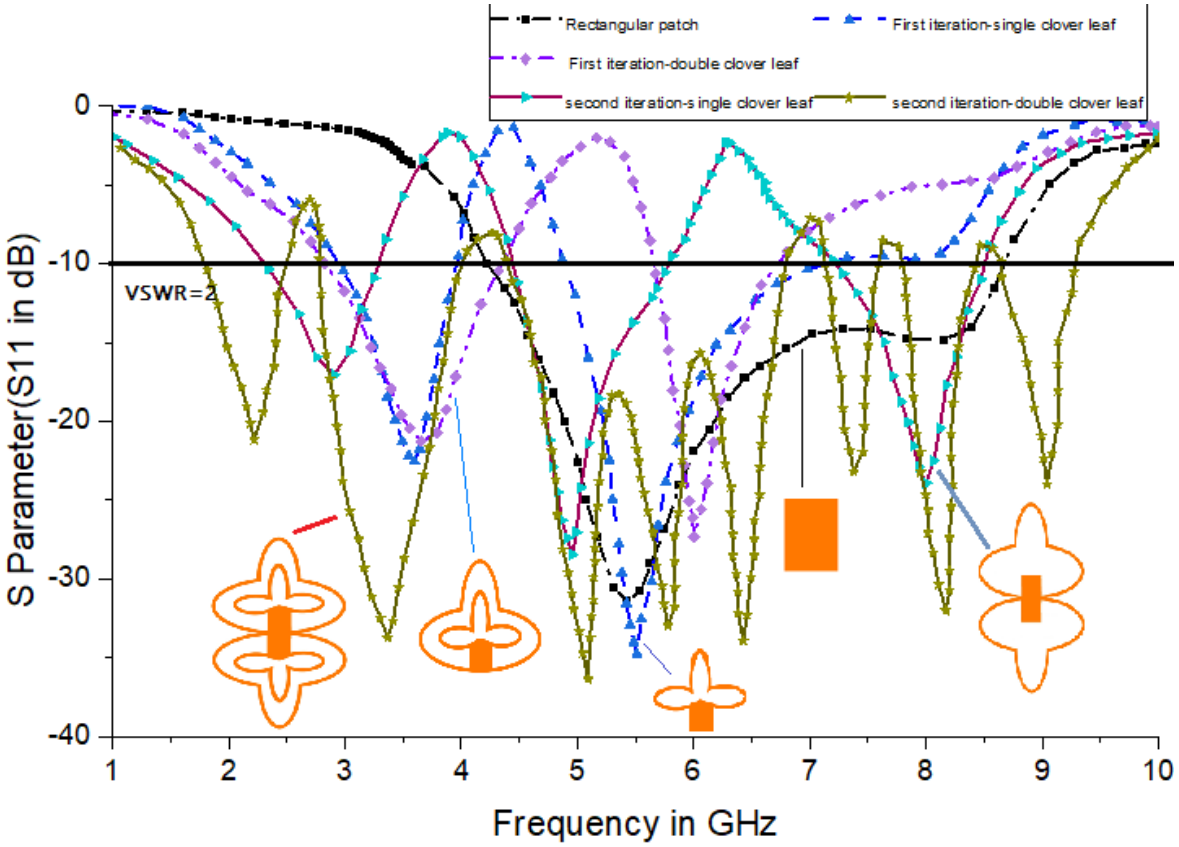

Fig 4. Reflection coefficient of antenna evolution (Step 1 to proposed design)

In this division, the proposed antenna efficiency analysis was likely with the use of the HFSS simulation software. Fig. 4displays a comparison of multiple iterations (iteration 1 & 2) of suggested clover leaf shaped fractal antennas with varied Insertion loss(S_{11}) responses. The resonance frequency is obviously sensitive to the fractal customary area CA parameter, and even a small deviancy from the ideal value can induce a band divergence. The operating frequency band that includes WLAN (5.15–5.825 GHz) and is illustrated graphically in Fig.4 corresponds to a rectangular patch antenna resonating at 5.42 GHz with an S11 of -31.547dB. A single clover-shaped antenna resonates the dual frequency range of (3-4.2) GHz and (5.3-6.4 GHz) during the first fractal iteration, equivalent to (3.3-3.6 GHz) for WiMAX band and (5.15-5.825 GHz) for WLAN applications. The ITU-R band (7.725-8.25 GHz) produces the third resonance mode by cloning the top double cover leaf with a phase difference of 180^0.The cloning procedure has no effect on the other resonances (ITU-R) generated in phases 1 and 2. Creating a single clover leaf over a rectangular patch repeats the initial iteration, as does cloning the single leaf to create a double clover leaf, the S11 responses of which have also been compared. The clover shaped ring is added during the second iteration, resulting in a fourth resonance mode with S11 of -24.66dB at the ITS band (5.795-6.4 GHz). The findings show that the frequency band of the inner resonance mode is unaffected by the outside signal path. The resonant band for WiMAX, WLAN, ITS band, and ITU-R band applications after the second iteration covers 2.3-3.3 GHz, 4.5-5.8 GHz, 5.8-6.8GHz, and 7.3-8.4 GHz..

Step Impedance Resonator (SIR) for Harmonics Supression:

A structural design of a proposed filtering antenna and a stepped impedance resonator network is shown in Fig. 5 and facilitate to suppress harmonic signals at wireless system end module. A Band Pass Filter(BPF) is used to achieve the proposed antenna's bandpass response and impedance. The bandwidth is also increased as a result of the additional reflection pole. The result of the high integration has been examined, and the results have been verified using numerical computations and full-wave simulations. The overall structure's dimensions were drastically lowered throughout this design. The antenna's filtering architecture includes half-wavelength parallel linked resonators, a patch element, and a micro strip line feed. Both the filter and the patch antenna share the centre inserted ground plane..

The suggested stub-loaded graduated impedance resonator construction is made up of three short-circuited stubs. Due to the resonator's symmetrical structure, it may be investigated using the concept of even modes and

odd modes. The proposed resonator's symmetrical structure with short-circuit stub and open-circuited stub at the end shunts halfway through the resonator is kept in the equivalent network of even and odd mode. As a result, we may revisit the circuits' odd- and even-mode analogues to even and odd mode theory. Each resonance is defined by a voltage distribution on the resonator which is either symmetric (even-mode) or asymmetric (odd-mode). The first higher order resonance occurs in an even mode, the basic resonance in an odd mode, and so on. The following are the requirements for determining a SIR's resonance frequencies:

$$\tan\theta_1 = K\cot\theta_2 \text{ (odd mode)} \quad (12)$$

$$\tan\theta_2 = -K\cot\theta_2 \text{ (even mode)} \quad (13)$$

where K is the impedance transformation ratio of the Stepped Impedance Resonator(SIR) defined as

$$K=\frac{Z_2}{Z_1}, \quad (14)$$

When K=1, $\theta_1+\theta_2=\pi/2$ at f_0.

Gap or tapped coupling can be used to connect the feed lines to the end resonators of a bandpass filter. When the latter is employed, a resonator's single loaded Q(Qsi) is calculated. The Band pass filter specification, which describes the bandpass response, should decide the value of Qsi. The value of Qsi for a tapped resonator is [5].

$$Q_{si}=R_L\frac{\omega_0}{2}\frac{dB}{d\omega}\Big|_{\omega_0} \quad (15)$$

Where, R_L is the resistive load of the resonators perceived by the feed line at the tap point, ω_0 is the operating frequency, and B is the total susceptance of the resonator as seen by the tap point's feed line. As a result, for the tapped SIR, Qsi can be calculated as follows.

When $0 < \phi < \theta_2$

$$\frac{Q_{si}}{R_L}=\frac{1}{2Z_2}\{\phi\sec^2(\phi)+\sec^2(\theta_2-\phi).\frac{(\theta_2-\phi)[R^2+g^2(\theta_2)]+R_h(\theta_2)}{[g(\theta_2)-R\tan(\theta_2-\phi)]^2}\} \quad \textbf{(16)}$$

where

$$g(\theta_2)=\frac{R-tan(\theta_2)\,tan(2\theta_1)}{tan(\theta_2)+R\,tan(2\theta_1)}$$

and

$$h(\theta_2)=\frac{\sec^2(2\theta_1)\{(2\theta_1)[\tan^2(\theta_2)+R^2]+R(\theta_2)\sec^2(\theta_2)\}}{[\tan(\theta_2)+R\tan(2\theta_1)]^2} \quad (17)$$

When $\theta_2 < \phi < \theta_1+\theta_2$

$$\frac{Q_{si}}{R_L}=\frac{1}{2Z_1}[g^2(p)h(p)+g^2(q)h(q)] \quad (18)$$

Where

$$p=2\theta_1+\theta_2-\phi$$

$$q=\phi-\theta_2$$

$$g(\zeta)=\frac{\sec(\zeta)}{R-\tan(\theta_2)\tan(\zeta)} \quad (19)$$

when the value of 1 is equal to the value of 2. If the tap point on the I/O SIRs can be flexibly slid, the transmission frequency zero may exist. The value of the SIRs, on the other hand, cannot be modified because it is defined by the filter specification.

Formulae and equivalent circuit of Filter Design

The following formulae and assumptions were used to create the given band pass filter. The filter was constructed with a -30 dB insertion loss, which aided in identifying the filter's order. Calculations were made using the following equations to determine L and C:

$$L=0.002l\left[\ln\left(\frac{2l}{w+t'}\right)+0.5+0.2235\left(\frac{2l}{w+t'}\right)\right] \quad (20)$$

$$C=\frac{A\varepsilon_0\varepsilon_r}{d} \quad (21)$$

Where, l, w and t are length, width of the substrate and thickness of the substrate, calculated from transmission line model of microstrip patch antenna

The band pass filter designed is a Butterworth filter for which the corresponding 'g' has been used to determine L, C components of the filter and finally determine the impedance values of each element. Using the below formula, 'N' can be determined.

$$\text{Insertion Loss, } I_L = 10\log_{10}(1+\Omega^{2N}) \quad (22)$$

Series inductor (L=g*Z) can be further simplified by,

$$\bar{L} = \frac{L}{\omega_U - \omega_L} \quad , \quad (23)$$

$$\bar{C} = \frac{\omega_U - \omega_L}{\omega_0^2 L} \quad (24)$$

Parallel capacitor(C=g/Z) can be estimated by,

$$\bar{C} = \frac{C}{\omega_U - \omega_L} \quad , \bar{L} = \frac{\omega_U - \omega_L}{\omega_0^2 C} \quad (25)$$

Bandwidth factor of the designed filter can be defined by using the following formula

$$bf = \tan\left(\frac{\pi}{2}\left(1 - \frac{s_{bw}}{2}\right)\right) \quad (26)$$

$$s_{bw} = \frac{\omega_U - \omega_L}{\omega_0^1}, \quad (27)$$

where,

$$\omega_0 = \frac{\omega_U + \omega_L}{2}$$

Where,

ω_U=designed filter's upper cut off frequency
ω_L=designed filter's lower cut off frequency

Impedance (series inductor),

$$Z = bf * g \quad (28)$$

Admittance (parallel capacitor),

$$Y = bf * g \quad (29)$$

Ω, ω_0= Cut off frequency
N = Number of elements in the filter
b*f* = Bandwidth factor
The characteristic impedance lines of the stepped impedance resonator are Z_1 and Z_2. Y_{in} is a distinct position's input admittance. The input admittance (Y_{in}) of SIR is derived by means of the following equation:

$$Y_{in} = \frac{(Z1 - Z2\tan\theta1\tan\theta2)}{[jZ1(Z1\tan\theta1 + Z2\tan\theta2)]} \quad (30)$$

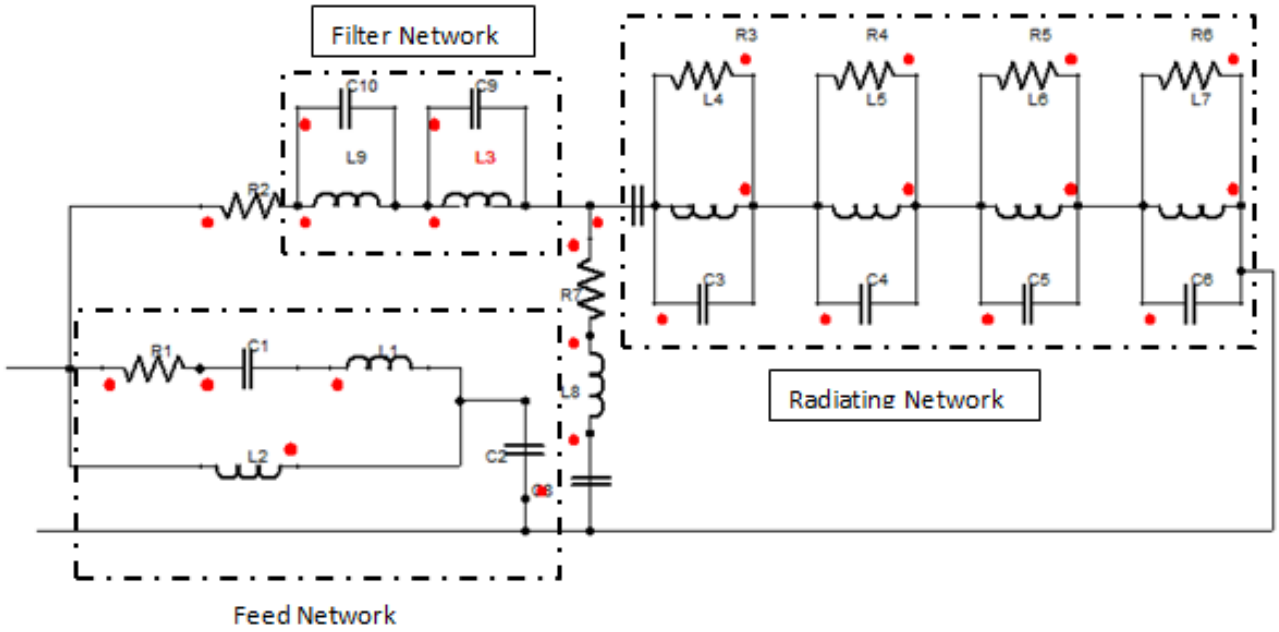

Figure 5 Equivalent circuit of proposed clover leaf shaped fractal antenna with SIR

Full-wave simulation was used to test the aforementioned theoretical conclusions, and the simulation results of a stepped impedance third-order 0.1-dB -Chebyshev filter response are shown in Fig. 6. f_1=3.3GHz, f_2=5.25GHz, f_3=5.9GHz, and f_4=7.9GHz are the filter's centre frequencies, respectively. The simulation S_{21} response of a SIR filter demonstrates individually controlled 3-dB relative bandwidth of 12%, 13.7%, 6.35%, and 7.8% for the centre frequencies of f_1, f_2, f_3, and f_4, respectively. In the stop band, a minimum attenuation level of -30 dB is attained for all of the centre frequencies shown in the insertion loss response. The SIR filter's response leads to the conclusion that it should be employed for the double clover shaped fractal antenna to eliminate spurious harmonics of $2f_0$, $3f_0$, $4f_0$, and so on.

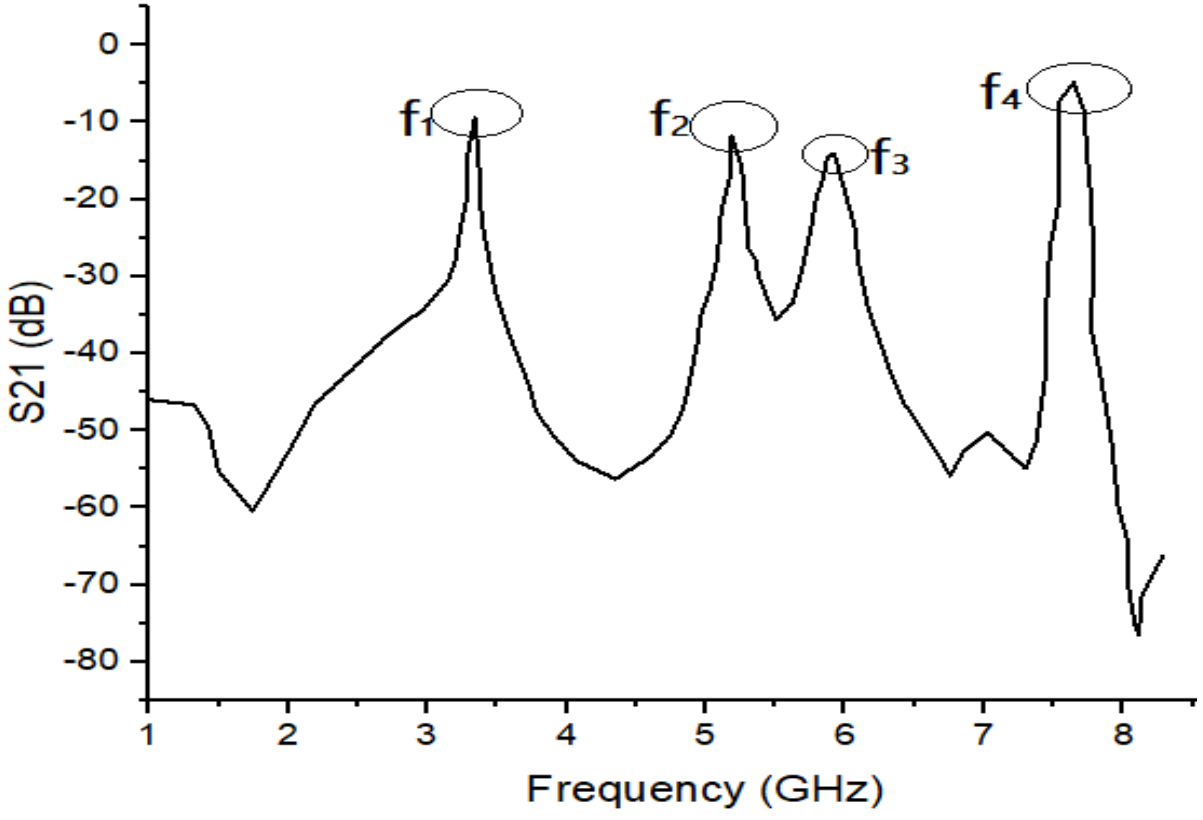

Fig. 6 Effect of Stepped Impedance filter parameters and its insertion loss response for the frequencies f_1, f_2, f_3, f_4

III. RESULTS AND DISCUSSION

Harmonics Suppression:

The superior harmonic suppression afforded by their intrinsically varied harmonic characteristics is one of the most notable features of this proposed antenna. The dipole based filtering network is a half-wavelength resonating filter having multiple harmonics at $2f_0$, $3f_0$, $4f_0$, and so on, with f_0 being the fundamental resonant frequency. On the other hand, the SIR may be act as a quarter-wave resonating filter with harmonics at $3f_0$, $5f_0$, and $7f_0$. When the SIR and the clover leaf fractal patch are concurrently adjusted to their resonating frequencies, harmonics at $2f_0$, $4f_0$ of even order may be virtually removed. The elimination of harmonics from the second iterated clover shaped antenna is shown in Fig. 8 at $1.8f_o$ (6.42GHz), $1.5f_o$(7.37GHz), and $1.73f_o$(9.04GHz), where f_0 is the fundamental resonating frequencies of 3.48GHz and 5.2GHz. Thereby, the proposed fractal antenna's gain and radiating efficiency are degraded by the lower order harmonics. Hence incorporating SIR filter with the proposed fractal antenna, overcomes the earlier degradation of peak gain. Fig. 7 shows the return loss of Clover shaped fractal antenna with and without SIR.

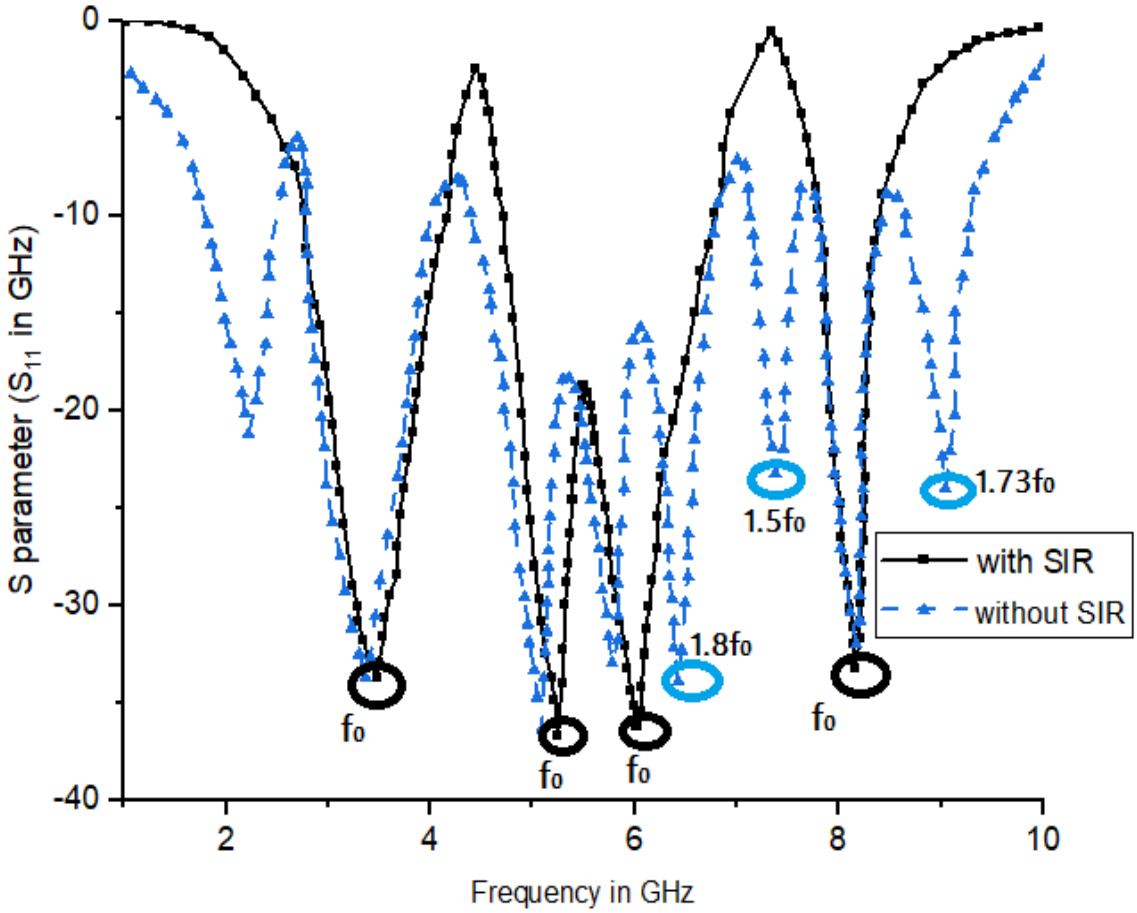

Fig. 7 Comparison of Return loss of Clover shaped fractal antenna with and without SIR

To verify the proposed design, an antenna prototype was constructed using ideal values and its performance was evaluated using an Vector Network Analyzer(VNA-Agilent's 8722ES). The minimal discrepancy between measured hardware and simulated results is due to fabrication tolerance and the SMA connection. The impedance bandwidth is 13% for a frequency band of 2.7 to 3.7 GHz and 12% for a frequency band of 5.1 to 6.6 GHz inside the relevant WiMAX and ITU-R bands. The observed peak gain of the proposed antenna for the desired band of frequencies is shown in Figure 12. The proposed antenna has a fair and adequate gain level

in these frequencies. Figure 8 illustrates the top and bottom perspectives of the built clover-shaped fractal antenna design.

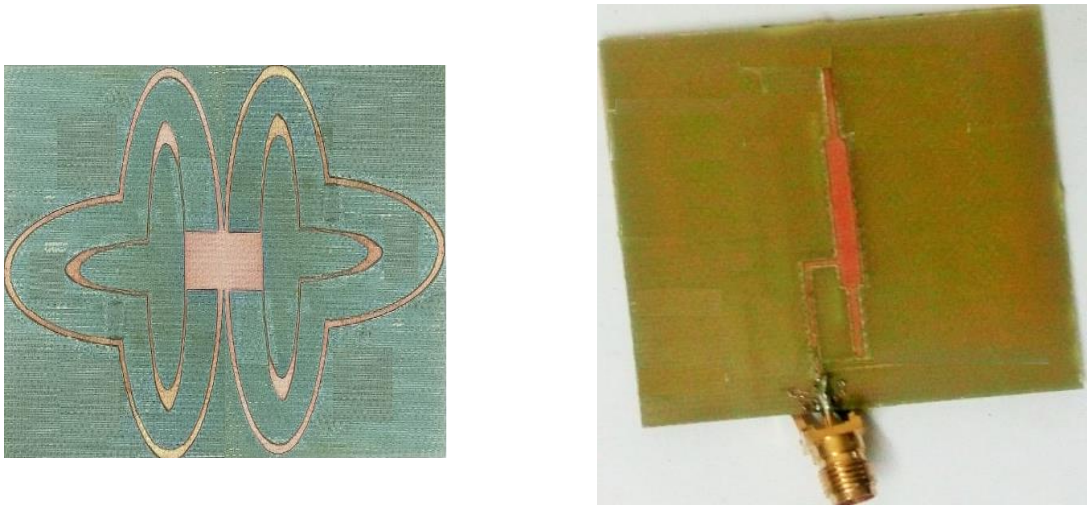

(a) (b)

Fig 8. Fabricated Prototype of the Clover shaped fractal antenna (a) Top perspective(b) Bottom perspective

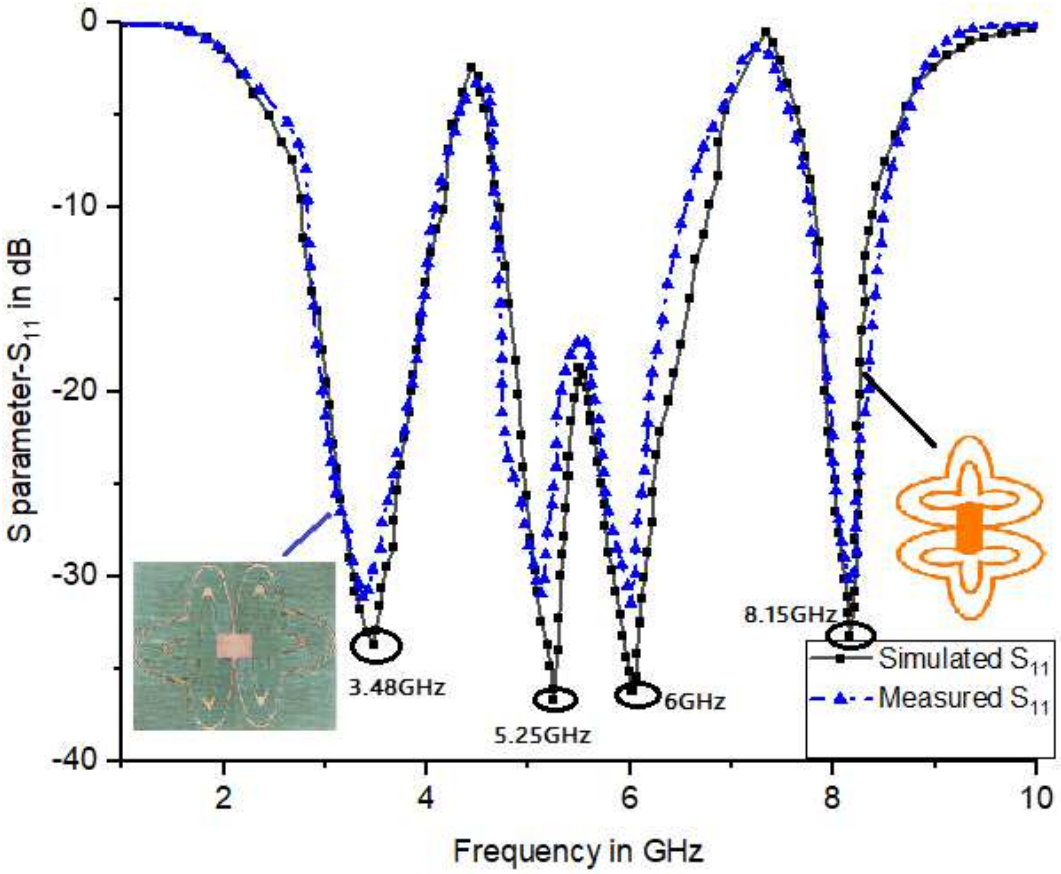

Fig.9 Performance Analysis of return loss of Proposed Fractal Antenna through Simulated and Measured Results

There is a little discrepancy between simulated and measured results, due to error in measurement or fabrication system. The effect of ground plane should be considered once the filtering antenna equipment in the system of RF front end. The performance of out of band and in-band continue to be unaffected as the ground plane is decreased or increased. The insertion and in-band return losses are good in this proposed design. The proposed antenna's measured and simulated returnloss are shown in Figure 9 which shows clear correlation

between measurement and simulation results. Measured results reveals that the return loss, S_{11} of -31.09dB at 3.36GHz, -30.91dB at 5.12GHz, -31.44dB at 6GHz , and -30.125dB, at 8.14GHz, which conform to the WiMAX, WLAN, ITS, and ITU-R frequency and impedance bandwidth standard criteria.

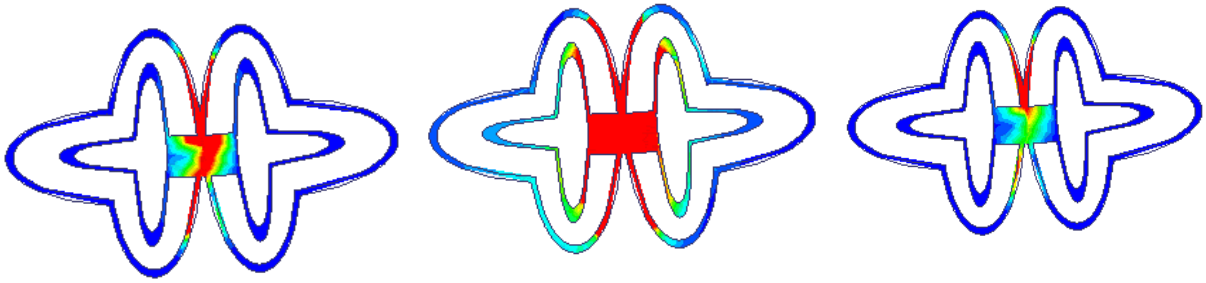

(a) (b) (c)

Fig 10 Current distribution at (a) 3.55 GHz (b)5.15 GHz (c) 8 GHz

Figure 10 depicts, the surface current distribution at 3.55GHz, 5.15 GHz, 8 GHz in the clover fractal area CA. The length of the existing route is 31 mm. At 3.5 GHz resonance arises due to the route length being near to $\boldsymbol{\lambda}_g/4$ (monopole antenna length). The xz-plane and the yz-plane corresponding to H-plane & E-plane are the two primary planes that represent the radiation patterns of designed antennas. Figures 11 shows the measured radiation patterns of the antenna at the centre frequency of each band. The measured left-handed circular polarised radiation patterns (LHCP) and right-handed circular polarised radiation patterns (RHCP) with phi $=0^0$ & 90^0 are shown in Fig. 11 for the WiMAX band at 3.5 GHz, the WLAN band at 5.75 GHz, the ITS band at 6.1 GHz, and the ITU-R band at 8 GHz.The antenna radiates Omni directionally in the Hplane, but only bi-directionally in the Eplane.

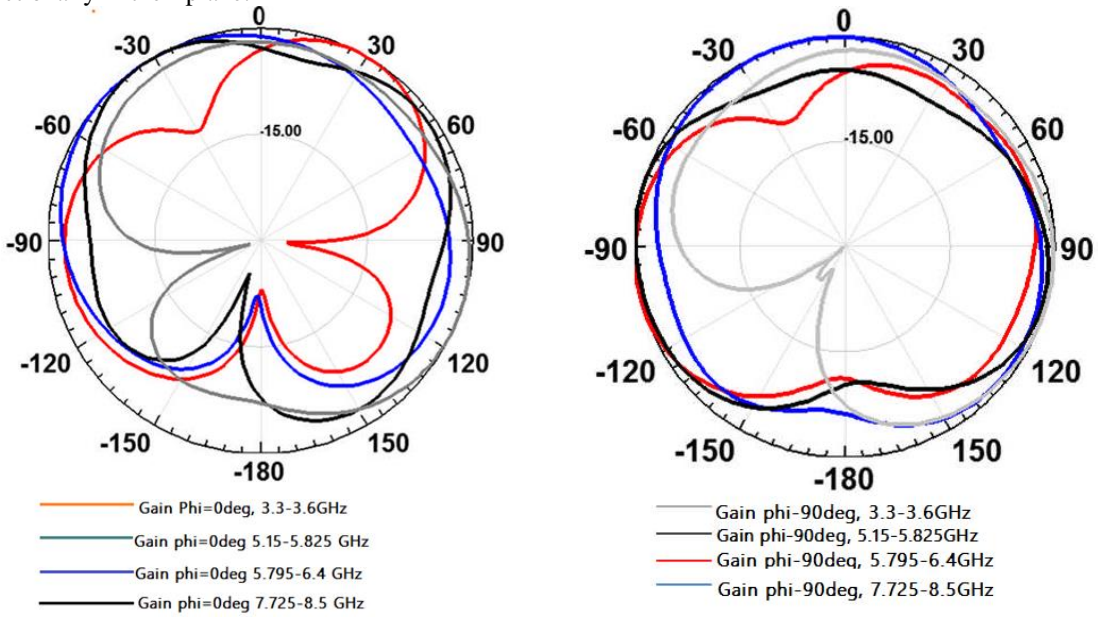

(a)

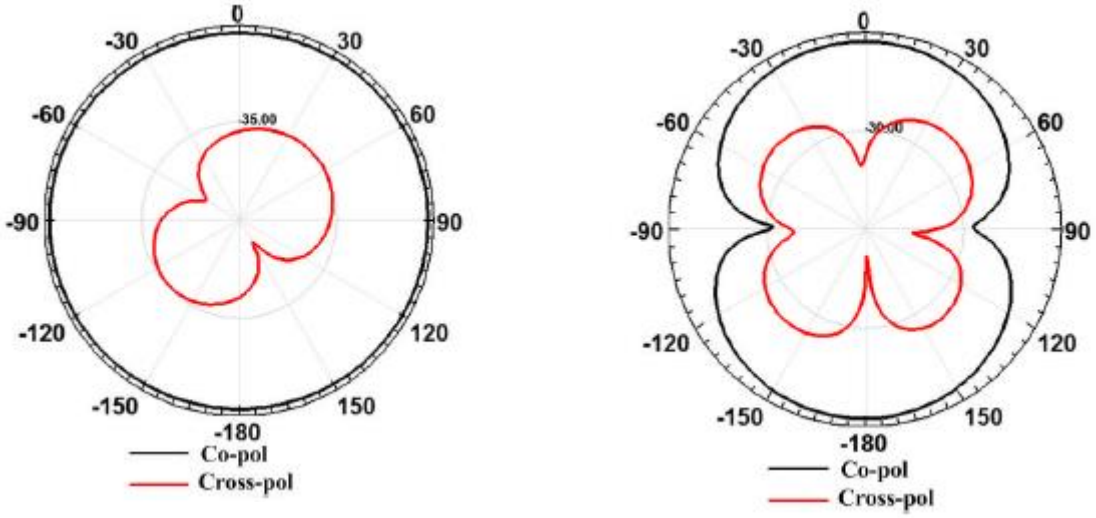

(b)

E Plane H Plane

Fig 11 Simulated and Measured 2D Radiation in E-plane and H-plane at (a)3.5GHz, 5.25GHz and 7.9GHz (b) 5.9 GHz

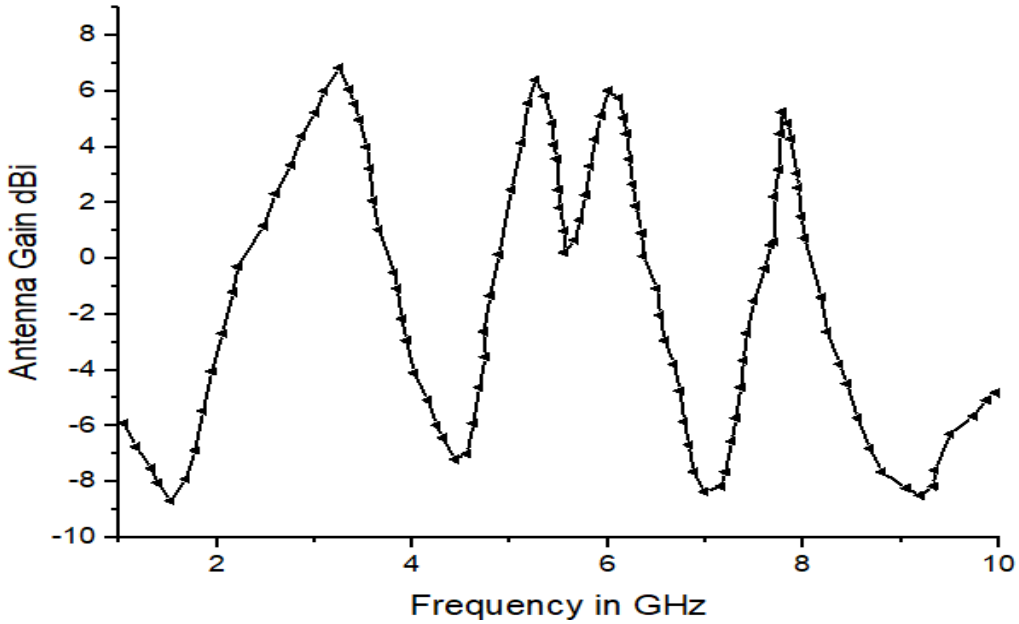

Fig 12 Gain Plot of the proposed stacked antenna

The frequency-gain plot for the proposed antenna is shown in Fig. 12, with peak gain of 7dBi at 3.5GHz, 6.5dBi at 5.25GHz, 6dBi at 5.9GHz, and 5.8dBi at 7.9GHz, the realized gain exceeds 4 dBi for all desired resonating frequencies. Despite a minor frequency offset between the measured and simulated values due to assembly/fabrication defects, good radiation performance and impedance matching are accomplished. From the perspective of realised gain, a quasi-filtering response is seen.

The comparative analysis of Proposed Fractal antenna with different iterations and structures is shown in Table 1. The performance comparison parameters include, Return loss, 10dB Bandwidth and Peak gain.

Table:1 Comparative analysis of Return loss, 10dB Bandwidth and Peak gain of Proposed Fractal antenna of different iterations

Antenna	Resonating Frequency	spurious	Return loss(dB)	10 dB-Bandwidt	Peak Gain

	range (range calculated @ -10dB) (GHz)-	harmonics rejection		h	(dBi)
Rectangular Patch(sim.)	5.42	-	-31.5457	-	2.4
First iteration-single clover leaf (sim.)	3-4.2	-	-22.5(@3.59 GHz)	800 MHz	3.2
	5.3-6.4	-	-34.75(@5.5 GHz)	1.1 GHz	2.8
First iteration-double clover leaf (sim.)	3.1-4	-	-21.2(@3.65 GHz)	900 MHz	3.5
	5-7	-	-26.1(@5.99GHz)	2 GHz	4.1
Second iteration-single clover leaf (sim.)	2.5-3.3	-	-17.3(@2.86 GHz)	800 MHz	3.6
	4.7-5.7	-	-28.45(@4.95 GHz)	1000 MHz	2.4
	6.7-8.7	-	-24.66(@7.99 GHz)	2 GHz	3.1
Second iteration-double clover leaf (without filter) (sim.)	2.2-3.3	-	-21.18(@2.21 GHz)	1100 MHz	5.1
			-33.73(@3.3 GHz)		5.1
	4.5-5.8	-	-36.34(@5.09 GHz)	1.3 GHz	3.5
			-32.96(@5.77 GHz)		3.5
	5.8-6.8	-	-33.92(@6.4 GHz)	1 GHz	4.5
	7.3-8.4	-	-23.21(@7.37 GHz)	1.1 GHz	4.3
			-31.99(@8.17 GHz)		4.3
	9.04		-23.99(@-23.99 GHz)	480 MHz	4.3
Second iteration-double clover leaf (with filter) (sim. & meas.)	3.3-3.6(sim.) 2.7-3.7(meas.)	$1.8f_0$	-33.73(@3.48GHz) -31.09(@3.36 GHz)	300 MHz	7
	5.15-5.825(sim.) 5.1-6.6(meas.)	$1.5f_0$	-36.69(@5.2 GHz) -30.91(@5.12 GHz)	675 MHz	6.5
	5.795-6.4(sim) 5.1-6.6(meas.)	$1.73f_0$	-36.25(@6.02 GHz) -31.44(@6 GHz)	605 MHz	6.2
	7.725-8.25(sim.) 6.8-8.4 (meas.)	absent	-33.20(@8.15 GHz) -30.125 (@8.14 GHz)	525 MHz	5.8

The different stages and iterations of designed Multiband clover leaf shaped fractal antenna stacked with Stepped Impedance Resonator has been depicted in Table 1, which illustrates the undesired lower order harmonics($1.8f_0$,$1.5f_0$, $1.73f_0$) has been suppressed and peak gain of greater than 5dBi has been achieved for all resonating modes. The table 2shows the comparative analysis of existing relevant patch antennas in literature with the proposed antenna which demonstrates the proposed antenna exhibits better return loss, 10 dB bandwidth, moreover harmonics and undesired resonance has been eliminated

Table 2: Comparison with some previous relevant filtering patch antennas in literature with proposed antenna

Ref.	Design Configuration	Integrated Filtering?	Frequency Range (GHz)	Return loss(dB) (@ Resonating Frequency,f_0)	Spurious rejection	10 dB-Bandwidth	Peak Gain (dBi)
[1]	Modified Ultra Wide Band array of antennas with a single-wing BPF filter	Yes	2.89 -9.94	-24.3(@6.5 GHz)	$1.5f_0$	7.05 GHz	5.2
[2]	filter with	Yes	2.38-2.5	-28(@2.44 GHz)	$2.3f_0$	120 MHz	4.5

	coupled open-loop microstrip line resonators.						
[3]	Integrating monopole patch antenna with an Inter-digital BPF	Yes	1.02 -1.92	-26(@2.44GHz)	$2.4f_0$	900 MHz	3.5
[4]	Monopole antenna with split ring resonator (SRR)	Yes	3.05 - 4.10 5.10 - 6.40 7.50 - 8.61	>-10(@3.575 GHz) -22.5(@5.75 GHz) -25(@8.01GHz)	$2\ f_0$	1050 MHz 1300 MHz 1110 MHz	3.4
[5]	Capacitive loaded loop (CLL) filter integrated with Planar filtering antenna	Yes	2.264-2.46	-31(@2.36 GHz)	$1.8f_0$	196 MHz	1.376
[6]	UWB slot antenna integrated with with SIR feed line and 2 ground slots	Yes	3.1 - 11	-24(@7 GHz)	$2\ f_0$	7.9 GHz	4
[7]	UWB antenna integrated with SRR BPF filter	Yes	2.95 - 10.82	-22(@6.883 GHz)	$3f_0$	7.89 GHz	4.25
[8]	A UWB filtering antenna using a microstrip circular patch antenna and a Multimode Resonator (MMR) built into a triangular ring stub	Yes	3.2-3.8 5.0-5.34, 5.5-6.4, 7.5-8.1	-15(@3.5 GHz) -19.5(@ 5.17 GHz) 21.8(@ 5.95 GHz) 19.4(@ 7.8 GHz)	$3.2f_0$	600 MHz 340 MHz 900 MHz 600MHz	4 3.25 2.4 3.8
[9]	filtering feed network for planar antenna array based on slots	Yes	3.15-3.45, 5.0-5.625, 5.6-6.2, 7.55-8.2	-16(@ 3.3 GHz) -25(@ 5.313 GHz) -24(@ 5.9 GHz) -21(@ 7.875 GHz)	-	300MHz 625 MHz 600 MHz 650 MHz	3.5 2.9 1.8
[10]	Filtering antennas stacked with E-shaped feeding lines	Yes	3- 3.95	-31(@3.5 GHz)	-	950 MHz	4.3
This Work	Proposed clover leaf fractal antenna integrated with Stepped Impedance resonator	Yes	3.3-3.6, 5.15-5.825, 5.795-6.4, 7.725-8.25	-33.73(@3.48GHz) -36.69(@5.2 GHz) -36.25(@6.02GHz) -33.20(@8.15GHz)	$1.8f_o$ $1.5f_o$ $1.73f_o$	300 MHz 675 MHz 605 MHz 525 MHz	7 6.5 6.2 5.8

From the table 2, the proposed clover leaf shaped fractal antenna integrated with Stepped Impedance resonator is matched with the state-of-art related works in terms of spurious rejection, Gain Bandwidth and peak gain. The comparative analysis shows that designed antenna is free from lower order harmonics with better radiation characteristics.

IV. CONCLUSION

In this paper, a filtering fractal antenna combined with a Stepped Impedance filtering network for suppressing harmonics and filtering applications is developed and examined in response to the requirement. An aperture coupled feeding clover leaf shaped fractal antenna operating simultaneously over several bands, including WiMAX, WLAN, ITS, and ITU-R, was described. In terms of dimesnions, the proposed antenna geometry is 50 × 50 × 2 mm^3**.** The performance of the proposed structure is verified by theoretical calculations and full-wave simulations. The antenna has an excellent matching between the radiating impedances across its operating bands, and it supports circular polarisation over the ITU-R band & WiMAX band, with a 3-dB axial-ratio impedance bandwidth of 97%, according to the measurements and having S_{11} of -33.73dB, -36.69 dB, -36.25dB and -33.20dB for WiMAX, WLAN, ITS and ITU-R bands with peak gain of 7dBi, 6.5dBi, 6.2dBi and 5.8dBi has been achieved. Measured results shows good coordination with the proposed structure having S_{11} of -31.09dB, -30.09 dB, -31.44dB and -30.125dB for WiMAX, WLAN, ITS and International Telecommunication Union Radio-communication (ITU-R)bands. Omnidirectional radiation pattern in the H-plane and almost bidirectional in the E-plane, the antenna's gain is stable throughout all of its operational frequencies. Due to its low insertion loss and strong gain, the antenna is excellent for multiband wireless systems that need low-profile antennas.

Abbreviations

WiMAX: Worldwide Interoperability for Microwave Access; WLAN: wireless local-area network; ITU-R :International Telecommunication Union Radio-communication; MMR: Multimode Resonator;

Declarations

Availability of data and materials

Data sharing not applicable to this article as no datasets were generated or analysed during the current study.

Competing interests

The authors declare that they have no competing interests

Funding

Not Applicable

Authors' contributions:

All authors contributed in designing the proposed schemes and also writing and reviewing the manuscript. The authors approved the final manuscript.

CONFLICTS OF INTEREST:

NOT APPLICABLE

Consent for publication

All authors have agree and given their consent for submission of this paper to Euraship Journal of Wireless Communications and Networking.

REFERENCES

[1]. Ahmed, S.; Kim Geok, T.; Alias, M.Y.; Hossain, F.; Alsariera, H.; Abdaziz, A.; Soh, P.J. A UWB Antenna Array Integrated with Multimode Resonator Bandpass Filter. *Electronics* **2021**, *10*, 607. https://doi.org/10.3390/electronics10050607

[2]. X. He, Y. Zhang, M. Du, and J. Xu, "Lightweight and compact high-gain filtering aperture antenna fabricated by three-dimensional printing technology," IEEE Antennas Wireless Propag. Lett., vol. 17, no. 7, pp. 1141-1144, Jul. 2018.

[3]. X. Yang, H. Luyen, S. Xu, and N. Behdad, "Design method for low-profile, harmonic-suppressed filter-antennas using miniaturized-element frequency selective surfaces," IEEE Antennas Wireless Propag. Lett., vol. 18, no. 3, pp. 427-431, Mar. 2019.

[4]. C.-W. Tong, H. Tang, J. Li, W.-W. Yang, and J.-X. Chen, “Differentially coplanar-fed filtering dielectric resonator antenna for millimeter-wave applications,” IEEE Antennas Wireless Propag. Lett., vol. 18, no. 4, pp. 786-790, Apr. 2019.
[5]. P. F. Hu, Y. M. Pan, X. Y. Zhang, and B. J. Hu, “A compact quasi-isotropic dielectric resonator antenna with filtering response,” IEEE Trans. Antennas Propag., vol. 67, no. 2, pp. 1294-1299, Feb. 2019.
[6]. W. Yang, Y. Zhang, W. Che, M. Xun, Q. Xue, G. Shen, and W. Feng, “A simple, compact filtering patch antenna based on mode analysis with wide out-of-band suppression,” IEEE Trans. Antennas Propag., vol. 67, no. 10, pp. 6244-6253, Oct. 2019.
[7]. C.-K. Lin, and S.-J. Chung, “A filtering microstrip antenna array,” IEEE Trans. Microw. Theory Tech., vol. 59, no. 11, pp. 2856-2863, Nov. 2011.
[8]. Y. Yusuf, and X. Gong, “Compact low-loss integration of high-Q 3-D filter with highly efficient antennas,” IEEE Trans. Microw. Theory Tech., vol. 59, no. 4, pp. 857-865, Nov. 2011.
[9]. Z. H. Jiang, M. D. Gregory, and D. H. Werner, “Design and experimental investigation of a compact circularly polarized integrated filtering antenna for wearable biotelemetric devices,” IEEE Trans. Biomed. Circuits Syst., vol. 10, no. 2, pp. 328-338, Apr. 2016.
[10]. C.-X. Mao, S. Gao, Y. Wang, Z. Wang, F. Qin, B. Sanz-Izquierdo, and Q.-X. Chu, “An integrated filtering antenna array with high selectivity and harmonics suppression,” IEEE Trans. Microw. Theory Tech., vol. 64, no. 6, pp. 1798-1805, Jun. 2016.
[11]. F.-C. Chen, H.-T. Hu, R.-S. Li, Q.-X. Chu, and M. J. Lancaster, “Design of filtering microstrip antenna array with reduced sidelobe level,” IEEE Trans. Antennas Propag., vol. 65, no. 2, pp. 903-908, Feb. 2017.
[12]. X. Guo, L. Zhu, J.-P. Wang, and W. Wu, “Wideband microstrip-to-microstrip vertical transitions via multiresonant modes in a slotline resonator,” IEEE Trans. Microw. Theory Tech., vol. 63, no. 6, pp. 1902-1909, Jun. 2015.
[13]. Sahu, B.; Singh, S.; Meshram, M.K.; Singh, S.P. "Integrated Design of Filtering Antenna with High Selectivity and Improved Performance for L-Band Applications", AEU Int. J. Electron. Commun. 2018, 97, 185–194. [CrossRef]
[14]. Cheng, W. Compact 2.4-GHz "Filtering Monopole Antenna Based on Modified SRR-Inspired High-Frequency-Selective Filter" Optik 2016, 127, 10653–10658. [CrossRef]
[15]. D. Anandkumar, R.G. Sangeetha, "Design and analysis of aperture coupled micro strip patch antenna for radar applications, International Journal of Intelligent Networks", Volume 1, 2020, Pages 141-147, ISSN 2666-6030, https://doi.org/10.1016/j.ijin.2020.11.002.
[16]. Tang, M.C.; Chen, Y.; Ziolkowski, R.W. "Experimentally Validated, Planar, Wideband, Electrically Small, Monopole Filtennas Based on Capacitively Loaded Loop Resonators", IEEE Trans. Antennas Propag. 2016, 64, 3353–3360. [CrossRef]
[17]. Yang, H.; Xi, X.; Zhao, Y.; Wang, L.; Shi, X. "Design of Compact Ultrawideband Slot Antenna With Improved Band-Edge Selectivity", IEEE Antennas Wirel. Propag. Lett. 2018, 17, 946–950. [CrossRef]
[18]. Tang, M.C.; Shi, T.; Ziolkowski, R.W. "Planar Ultrawideband Antennas with Improved Realized Gain Performance" IEEE Trans. Antennas Propag. 2016, 64, 61–69. [CrossRef]
[19]. Sahu, B.; Singh, S.; Meshram, M.K.; Singh, S.P. "A New Compact Ultra-Wideband Filtering Antenna with Improved Performance" J. Electromagn. Waves Appl. 2018, 33, 107–124. [CrossRef]
[20]. Sahoo, A.K.; Gupta, R.D.; Parihar, M.S. "Highly selective integrated filter antenna for UWB application", Microw. Opt. Technol. Lett. 2017, 59, 1032–1037. [CrossRef]
[21]. Zhang, C.X.; Zhuang, Y.Q.; Zhang, X.K.; Hu, L.Z. "An UWB Microstrip Antenna Array with Novel Corporate-Fed Structure", Prog. Electromagn. Res. C 2014, 52, 7–12. [CrossRef]
[22]. Li, Y.; Zhao, Z.; Tang, Z.; Yin, Y. "Differentially-Fed, Wideband Dual-Polarized Filtering Antenna With Novel Feeding Structure for 5G Sub-6 GHz Base Station Applications" IEEE Access 2019, 7, 184718–184725. [CrossRef]
[23]. A. Potapov, "Fractal Electrodynamics: Numerical Modeling of Small Fractal Antenna Devices and Fractal 3D Microwave Resonators for Modern Ultra-Wideband or Multiband Radio Systems," Journal of Communications Technology and Electronics, vol. 64, pp. 629-663, 2019.
[24]. S. Jindal, J. S. Sivia, and H. S. Bindra, "Hybrid fractal antenna using meander and Minkowski curves for wireless applications," Wireless Personal Communications, vol. 109, pp. 1471-1490, 2019.
[25]. X. Bai, J.-w. Zhang, and L.-j. Xu, "A broadband CPW fractal antenna for RF energy harvesting," in 2017 International Applied Computational Electromagnetics Society Symposium (ACES), 2017, pp. 1-2.
[26]. A. Gupta, H. D. Joshi, and R. Khanna, "An X-shaped fractal antenna with DGS for multiband applications," International Journal of Microwave and Wireless Technologies, vol. 9, p. 1075, 2017.
[27]. M. Naser-Moghadasi, R. A. Sadeghzadeh, R. Khajeh Mohammad Lou, B. S. Virdee, and T. Aribi, "Semi fractal three leaf clover-shaped CPW antenna for triple band operation," International Journal of RF and Microwave Computer-Aided Engineering, vol. 25, pp. 413-418, 2015.
[28]. P. F. da Silva Junior, M. S. P. Silva Filho, E. E. de Carvalho Santana, P. H. da Fonseca Silva, E. E. C. de Oliveira, M. A. de Oliveira, et al., "Fractal and Polar Microstrip Antennas and Arrays for Wireless Communications," in Wireless Mesh Networks-Security, Architectures and Protocols, ed: IntechOpen, 2019.
[29]. S. Denis, C. Person, S. Toutain, S. Vigneron, and B. Theron, “Improvement of global performances of band-pass filters using nonconventional stepped impedance resonators,” in 28th Eur. Microwave Conf. Dig., 1998, pp. 323–328.
[30]. C. Quendo, E. Rius, C. Person, and M. Ney, “Integration of optimized low-pass filters in a bandpass filter for out-of-band improvement,” IEEE Trans. Microwave Theory Tech., vol. 49, pp. 2376–2383, Dec. 2001.

[31]. M. Matsuo, H. Yabuki, and M. Makimoto, “The design of a half-wavelength resonator BPF with attenuation poles at desired frequencies,” in IEEE MTT-S Int. Microwave Symp. Dig., 2000, pp. 1181–1184.
[32]. H. Zhangfang, X. Wei, L. Yuan, H. Yinping, and Z. Yongxin, "Design of a modified circular-cut multiband fractal antenna," The Journal of China Universities of Posts and Telecommunications, vol. 23, pp. 68-75, 2016.
[33]. M. Gupta and V. Mathur, "Wheel shaped modified fractal antenna realization for wireless communications," AEU-International Journal of Electronics and Communications, vol. 79, pp. 257-266, 2017.
[34]. Palanisamy, S.; Thangaraju, B.; Khalaf, O.I.; Alotaibi, Y.; Alghamdi, S.; Alassery, F. A Novel Approach of Design and Analysis of a Hexagonal Fractal Antenna Array (HFAA) for Next-Generation Wireless Communication. Energies 2021, 14, 6204. https://doi.org/10.3390/en14196204
[35]. O.-Y. Kwon, R. Song, and B.-S. Kim, "A fully integrated shark-fin antenna for MIMO-LTE, GPS, WLAN, and WAVE applications," IEEE Antennas and Wireless Propagation Letters, vol. 17, pp. 600-603, 2018.
[36]. H. Wang, L. Liu, Z. Zhang, Y. Li, and Z. Feng, "A wideband compact WLAN/WiMAX MIMO antenna based on dipole with V-shaped ground branch," IEEE Transactions on Antennas and Propagation, vol. 63, pp. 2290-2295, 2015.
[37]. Palanisamy, S.; Thangaraju, B.; Khalaf, O.I.; Alotaibi, Y.; Alghamdi, S. Design and Synthesis of Multi-Mode Bandpass Filter for Wireless Applications. Electronics 2021, 10, 2853. https://doi.org/10.3390/electronics10222853
[38]. A. Biswas and V. R. Gupta, "Design and Development of Low Profile MIMO Antenna for 5G New Radio Smartphone Applications," Wireless Personal Communications, pp. 1-12, 2019.
[39]. M. Ihamji, E. Abdelmounim, H. Bennis, M. Hefnawi, and M. Latrach, "Design of compact tri-band fractal antenna for RFID readers," International Journal of Electrical and Computer Engineering, vol. 7, p. 2036, 2017.
[40]. Kumar, P. Satheesh, P. Chitra, and S. Sneha. "Design of Improved Quadruple-Mode Bandpass Filter Using Cavity Resonator for 5G Mid-Band Applications." Future Trends in 5G and 6G: Challenges, Architecture, and Applications (2021): 219.
[41]. A. Desai, T. K. Upadhyaya, R. H. Patel, S. Bhatt, and P. Mankodi, "Wideband high gain fractal antenna for wireless applications," Progress In Electromagnetics Research, vol. 74, pp. 125-130, 2018.
[42]. M. Harbadji, T. A. Denidni, and A. Boufrioua, "Miniaturized dual-band fractal antenna with omnidirectional pattern for WLAN/WiMAX applications," Progress In Electromagnetics Research, vol. 70, pp. 31-38, 2017.
[43]. Y. B. Chaouche, I. Messaoudene, I. Benmabrouk, M. Nedil, and F. Bouttout, "Compact coplanar waveguide-fed reconfigurable fractal antenna for switchable multiband systems," IET Microwaves, Antennas & Propagation, vol. 13, pp. 1-8, 2018.
[44]. C. Elavarasi and T. Shanmuganantham, "SRR loaded periwinkle flower shaped fractal antenna for multiband applications," Microwave and Optical Technology Letters, vol. 59, pp. 2518-2525, 2017.
[45]. C. X. Mao, S. Gao, Y. Wang, B. Sanz-Izquierdo, Z. Wang, F. Qin, et al., "Dual-band patch antenna with filtering performance and harmonic suppression," IEEE Transactions on Antennas and Propagation, vol. 64, pp. 4074-4077, 2016.

Figure Title and Legend Section

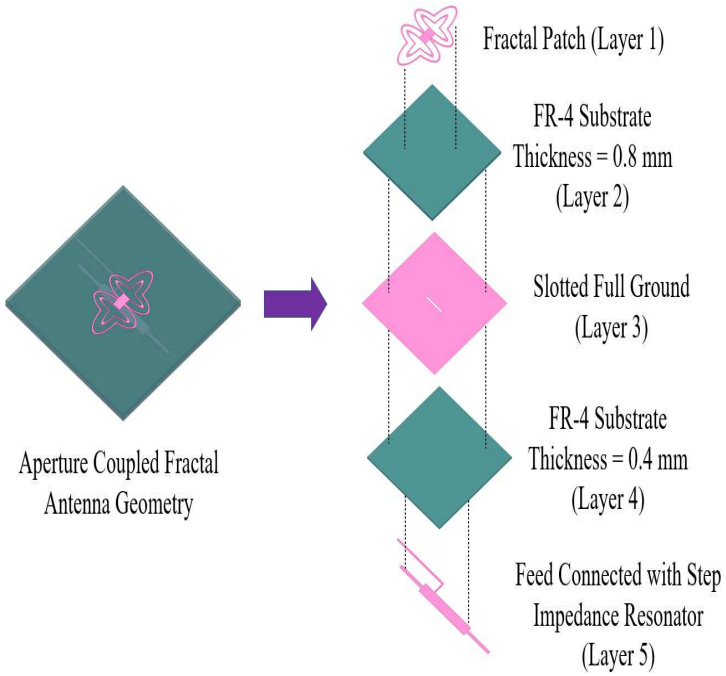

Fig.1 Layered structure of the proposed antenna

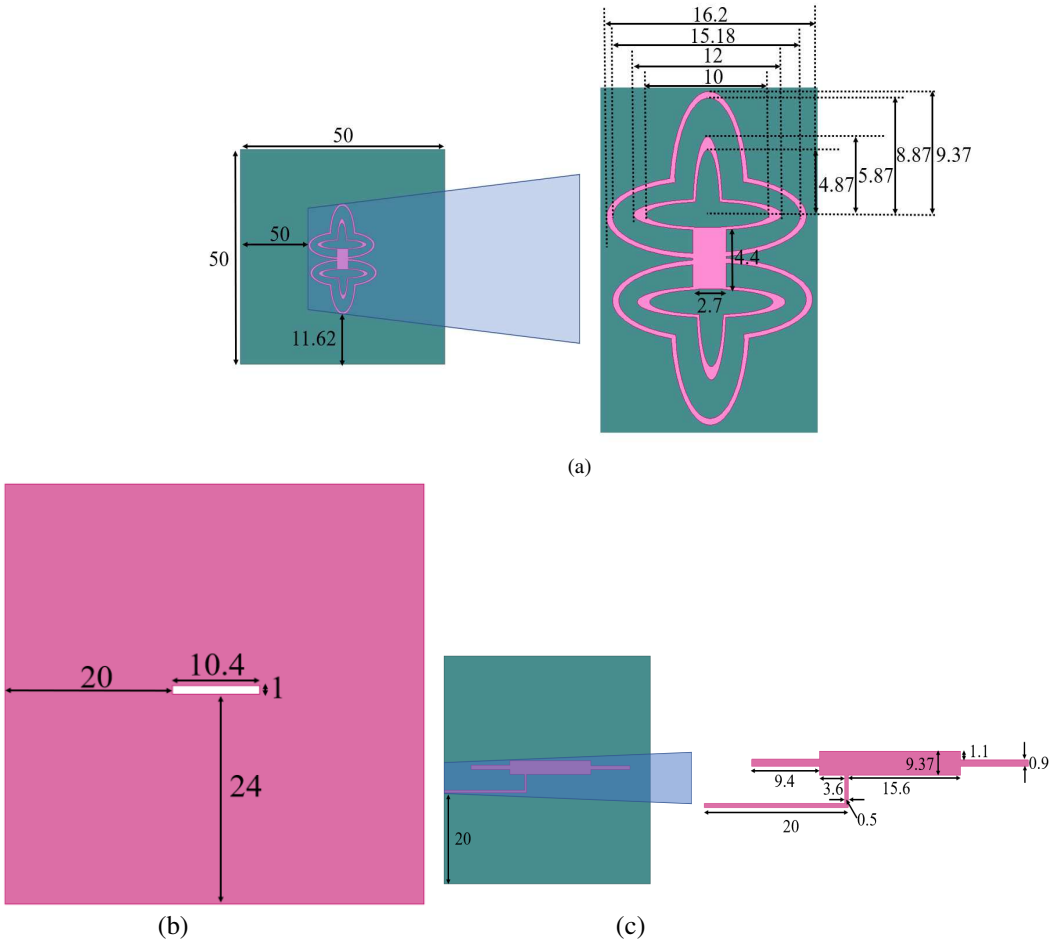

Fig 2. Antenna Geometry (a) Layered View (b) Layer 1 and 2 (c) Layer 3 (d) Layer 4 and 5

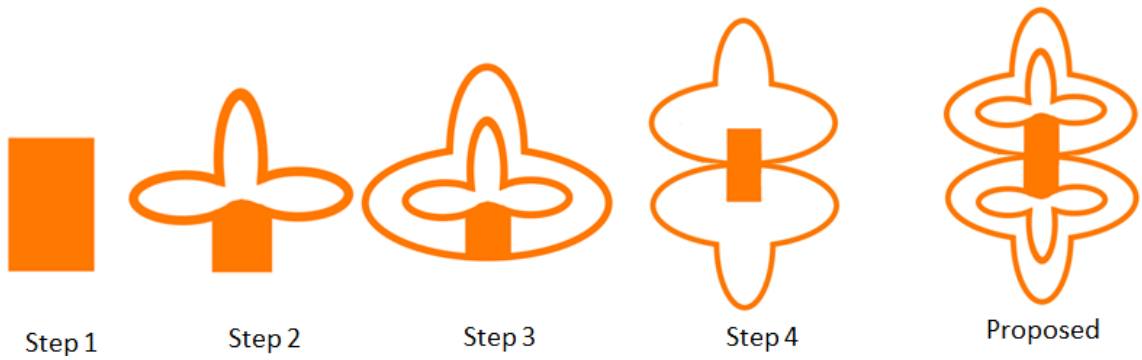

Fig 3. Evolution of proposed antenna

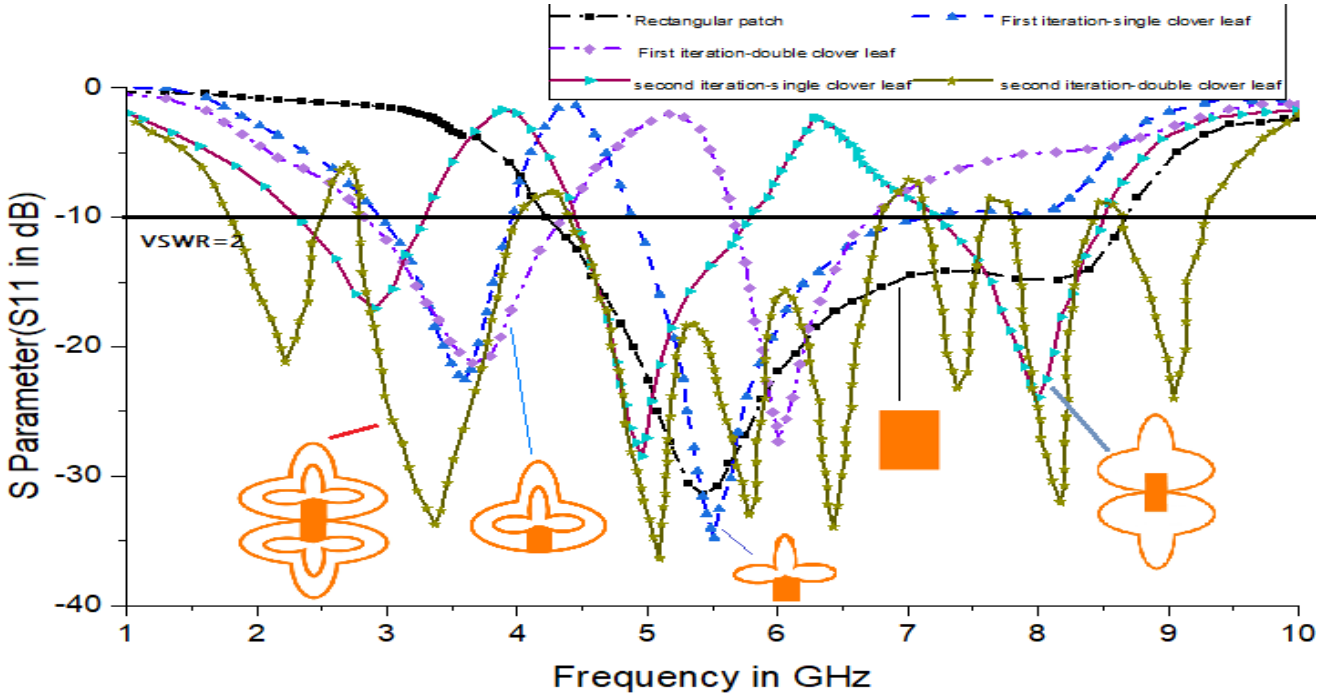

Fig 4. Reflection coefficient of antenna evolution (Step 1 to proposed design)

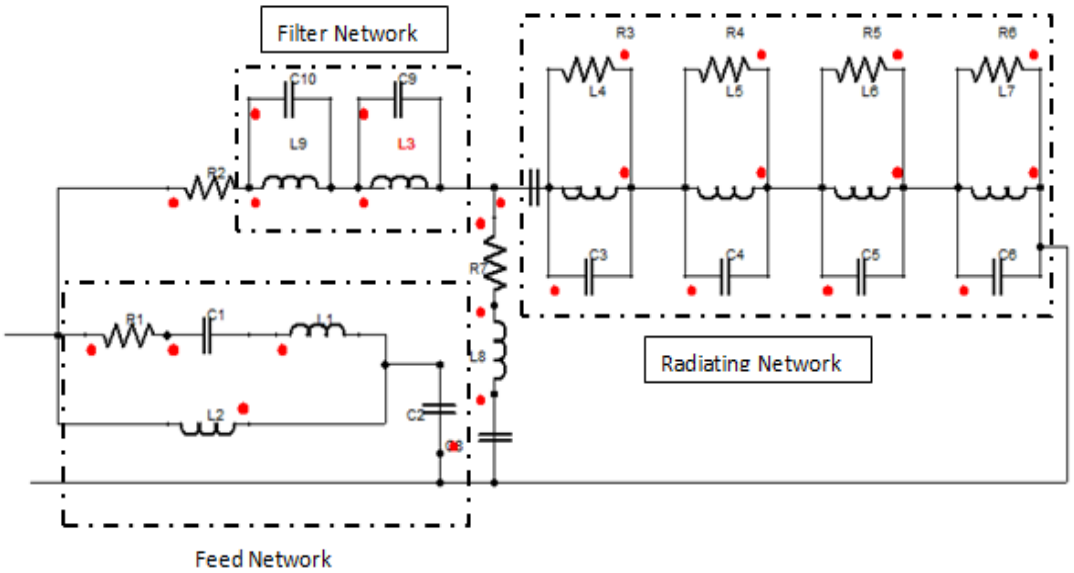

Figure 5 Equivalent circuit of proposed clover leaf shaped fractal antenna with SIR

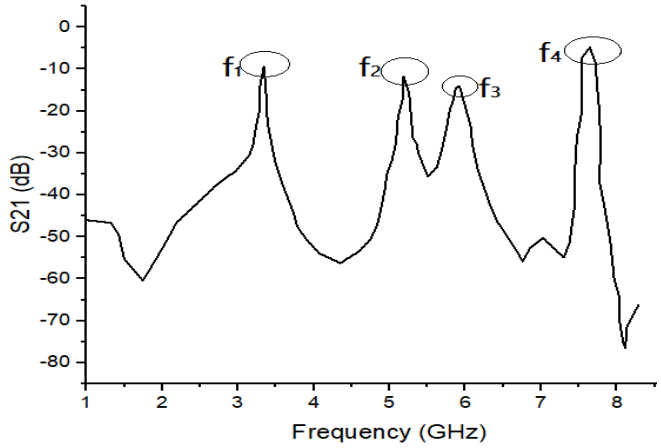

Fig. 6 Effect of Stepped Impedance filter parameters and its insertion loss response for the frequencies f_1, f_2, f_3, f_4

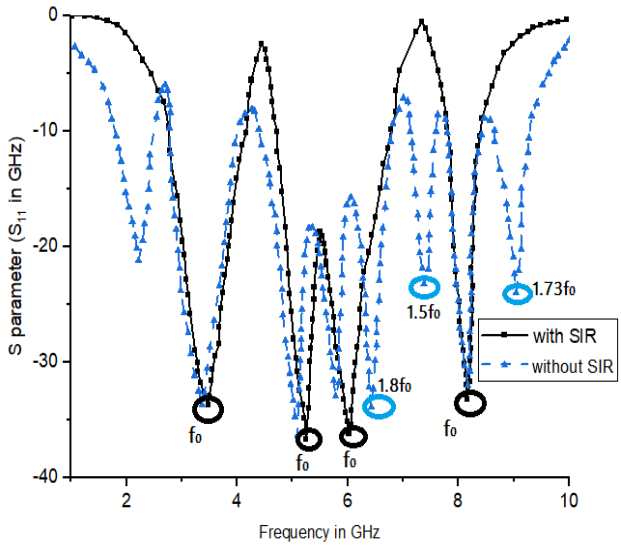

Fig. 7 Comparison of Return loss of Clover shaped fractal antenna with and without SIR

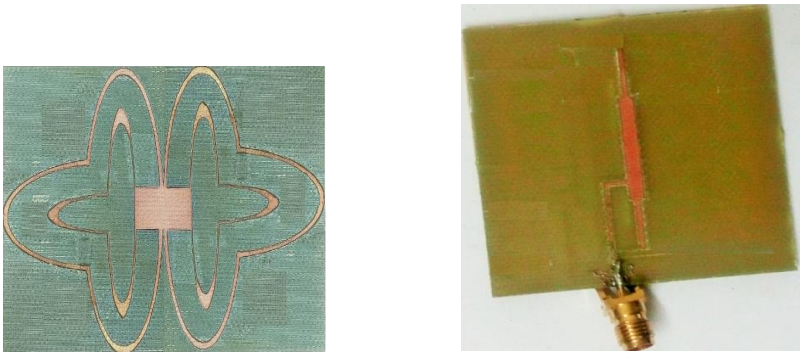

(a) (b)

Fig 8. Fabricated Prototype of the Clover shaped fractal antenna (a) Top perspective(b) Bottom perspective

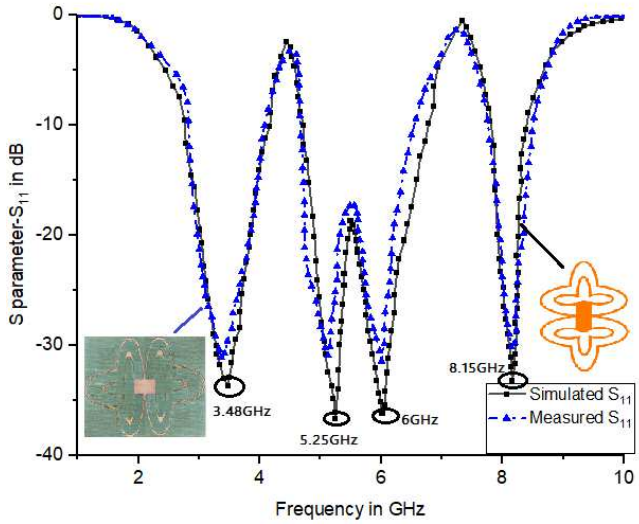

Fig.9 Performance Analysis of return loss of Proposed Fractal Antenna through Simulated and Measured Results

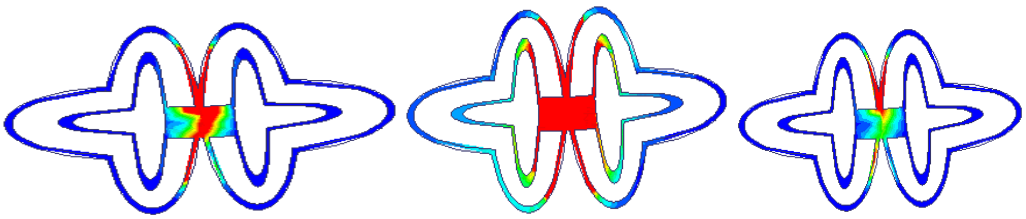

(a) (b) (c)

Fig 10 Current distribution at (a) 3.55 GHz (b)5.15 GHz (c) 8 GHz

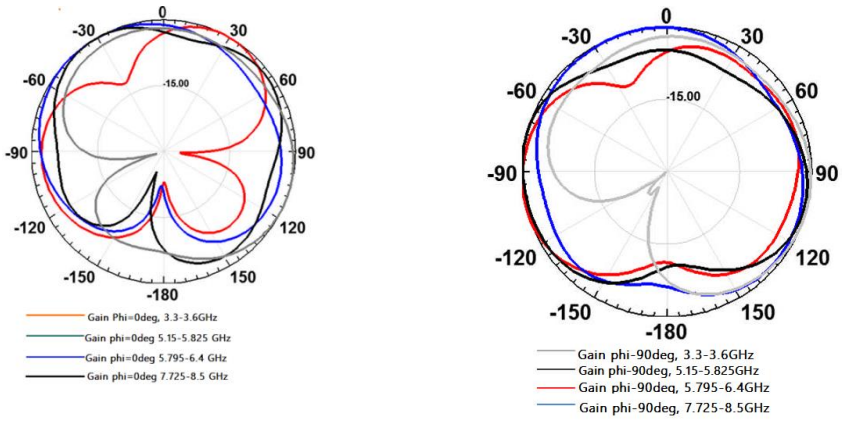

(a)

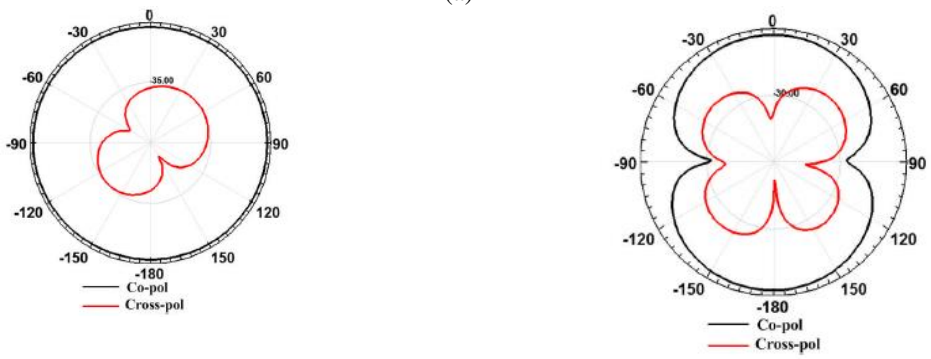

(b)

E Plane H Plane

Fig 11 Simulated and Measured 2D Radiation in E-plane and H-plane at (a)3.5GHz, 5.25GHz and 7.9GHz (b) 5.9 GHz

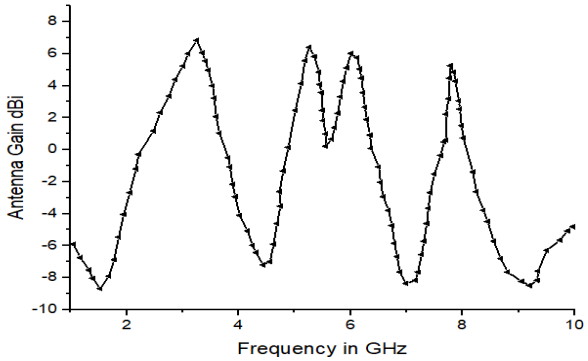

Fig 12 Gain Plot of the proposed stacked antenna